Deep-ultraviolet cavity ringdown spectroscopy

Sneep, M.C.; Hannemann, S.; van Duijn, E.J.; Ubachs, W.M.G.

published in
Optics Letters
2004

DOI (link to publisher)
10.1364/OL.29.001378

document version
Publisher's PDF, also known as Version of record

Deep-ultraviolet cavity ringdown spectroscopy

M. Sneep, S. Hannemann, E. J. van Duijn, and W. Ubachs

Laser Centre, Department of Physics and Astronomy, Vrije Universiteit, De Boelelaan 1081, 1081 HV Amsterdam, The Netherlands

Received January 20, 2004

The sensitive optical detection technique of cavity ringdown spectroscopy is extended to the wavelength range 197–204 nm. A novel design narrowband Fourier-transform-limited laser is used, and the technique is applied to gas-phase extinction measurements in CO_2, SF_6, and O_2. Further demonstration of the system capabilities is given in high-resolution recordings of the Schumann–Runge (0, 0), (1, 0), and (2, 0) bands in O_2.

OCIS codes: 120.6200, 300.1030, 300.6540.

Since the discovery of cavity ringdown spectroscopy (CRDS),[1] this sensitive optical technique has been applied to direct absorption monitoring in a wide wavelength range, spanning from the infrared range at 10 μm,[2] via the entire visible domain, to the UV. This broadness of wavelength range makes the technique applicable for gas-phase studies in cells, molecular beam jets, etching plasma reactors, laser photolysis, flames, furnaces and heat pipe ovens, hollow-cathode discharges, slit nozzle discharges, and diamond-depositing flames. For an overview of such applications we refer to Berden *et al.*[3] At the UV end of the spectrum CRDS was applied to detect the methyl radical in a hot filament reactor at $\lambda = 216$ nm,[4] and detection of ammonia molecules via an absorption feature at $\lambda = 205$ nm marks the cutting edge of CRDS at short wavelengths.[5] The sensitivity of CRDS is known to scale with $(1 - \mathcal{R})$, where $\mathcal{R}$ is the reflectivity of the mirrors forming the cavity; lower reflectivities decrease the number of round trips and thereby the time span over which an optical decay transient can be recorded. Production of mirrors that are highly reflective deeper into the UV becomes gradually more difficult. State-of-the-art reflectivities measure $\mathcal{R} \approx 96$–98% at deep-UV wavelengths. Here we report on extending the domain of CRDS beyond the 200-nm threshold into the deep UV, with applications to extinction, Rayleigh scattering, resonant absorption, and predissociative decay of small gas-phase molecules.

Wavelength-tunable laser pulses in the range 197–204 nm are produced by a Ti:sapphire (Ti:S) oscillator cavity that is pumped by the green output of a seeded Nd:YAG Q-switched laser and injection-seeded by the continuous-wave (cw) output of a Ti:S laser. The oscillator cavity contains no other elements than the Ti:S crystal; its cavity length is stabilized to the mode of the cw laser via the Hänsch–Couillaud locking scheme. On pumping at ~10 mJ/pulse the cavity delivers near-IR pulses at 1 mJ/pulse, at a duration of 15–24 ns and a 10-Hz repetition rate and in a bandwidth of ~50 MHz. The pulse duration is physically determined by the rate of stimulated emission in Ti:S and is a function of pump power and of the reflectivity of the output coupler, which for these measurements was taken at ~90%. Although we demonstrated that it is possible to amplify the output pulses to a level of 30 mJ/pulse in a bow-tie amplifier, for the present application this option is not employed. The effective fourth harmonics of these pulses are produced by consecutive frequency-mixing processes in three β-barium borate (BBO) crystals cut at the appropriate angles for type I phase matching. Finally, tunable narrowband deep-UV pulses of approximately 0.1–30 μJ of 8-ns duration and a bandwidth of 100 MHz are produced that are implemented in the CRDS setup. The bandwidth in the UV was calibrated by resonantly probing Yb atoms in a highly collimated beam by laser-induced fluorescence.

The CRD configuration is composed of two highly reflective mirrors (Rocky Mountain Instruments; radius of curvature, 1 m) forming a sealed cavity of length 86 cm. The measured ringdown time in an evacuated cavity is 90–100 ns, corresponding to a reflectivity of 97%. The cell can be evacuated by a turbomolecular pump, and gas can be inserted via a needle valve, allowing for controlled-pressure ramp scans as in previous CRDS measurements in the visible domain.[6] The experimental configuration, including the laser setup and the ringdown geometry, is depicted schematically in Fig. 1.

Using a digital oscilloscope (LeCroy WaveRunner LT342, with a sampling speed of 500 Msamples/s) we record CRDS decay transients and transfer them to a computer for further analysis. The decay time (1/e)

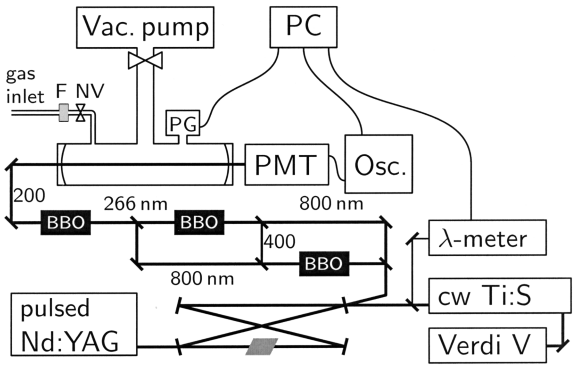

Fig. 1. Layout of the laser system delivering tunable-wavelength Fourier-transform-limited pulses in the range 197–204 nm and the CRD setup. Osc., digital storage oscilloscope; PMT, photomultiplier tube; PG, pressure gauge; NV, needle valve; F, aerosol filter.

0146-9592/04/121378-03$15.00/0

of an empty cell is of the order of 100 ns, whereas in extinction measurements transients as short as 40 ns are allowed by the analysis software. A laser pulse duration of 8 ns might produce a systematic deviation in the estimated decay rate, but calculation of the convolution integral shows that the resulting deviation is less than 1% if decay transients of $4.5\tau_{\mathrm{cav}}$ are used, as long as the fitting starts after the end of the pulse. The narrow bandwidth of the laser has the advantage that slit function effects that cause underestimation of the absolute extinction cross section in CRDS[5,7] do not play a role in the present investigation, not even when narrow lines are recorded; the linewidth of 100 MHz is much lower than the Doppler broadening of 3.3 GHz for O_2 at these short wavelengths. For an interpretation of ringdown transients in terms of a Beer's law exponential extinction one must ensure that the measured transients follow a monoexponential decay function. For this reason an alignment procedure was applied that optimizes the cavity for minimum deviation from a single exponential decay.[7]

By use of a pressure-ramp method,[6] the extinction cross sections of various gases can be determined. To avoid turbulence, we slowly fill the cell to 10^5 Pa over a time span of ~15 min, and during this time the cavity decay rate is continuously monitored. Three of these pressure scans are displayed in Fig. 2 for various gases. Each data point corresponds to the decay rate of an average over five measured decay transients. Since the loss rate corresponds to $\beta_0 + N\sigma_\lambda$, where β_0 is the empty cavity loss rate; the slope in the pressure curves is proportional to the extinction cross section σ_λ of the gas. Small differences in the intercepts in Fig. 2 may occur, representing small differences in the mirror reflectivity as a result of cleaning of the mirrors and of the time interval over which the cell has been evacuated. From fits to this slope the extinction cross sections are derived, the results of which are listed in Table 1 for CO_2 and SF_6. All measurements were performed at room temperature, and the ideal gas law was applied to convert pressure into density N. The indicated errors follow from a weighted average over several pressure scans, with the weights derived from the fit of the decay transient and a subsequent fit to the pressure ramp, and are 1σ estimates.

The observed extinction in CO_2 is largest. Ogawa[8] investigated the absorption cross section of CO_2 in the region 172–216 nm and found a weak but complicated band structure, superimposed on an underlying dissociative continuum. Our measurement of an extinction cross section at one specific wavelength (λ = 197.99 nm) agrees with the lower resolution value; future work employing the narrow bandwidth and the tunability of the deep-UV laser system may help to unravel the onset of band structures in CO_2 at 198 nm.[8]

For SF_6 the extinction is expected to be determined by Rayleigh scattering. In SF_6 only two measurements of a refractive index exist in the visible and the near-IR range.[9] Conversion into a cross section via $\sigma_\lambda{}^{\mathrm{R}} = 8\pi^3(n_\lambda{}^2 - 1)^2 F_{\mathrm{k}}(\lambda)/(3N^2\lambda^4)$ and the assumption of King factors $F_{\mathrm{k}}(\lambda)$ of this spherical molecule to equal unity give good agreement even in extrapolation to the deep UV.

The continuous tunability of the novel deep-UV laser system was employed in the recording of the spectra of three Schumann–Runge (SR) bands in O_2, parts of which are displayed in Fig. 3. This is, to our knowledge, the first time that the triplet-spin structure in the weakest (0, 0) band has been resolved. These measurements allow an accurate determination of the spin-state-dependent effects in the spectra and in the predissociation rates in the $B\,^3\Sigma_u^-, v' = 0$ state, as well as an assessment of the competition between fluorescent decay and predissociation. The combination of the narrow-bandwidth laser and the generation of exact fourth harmonics yields a

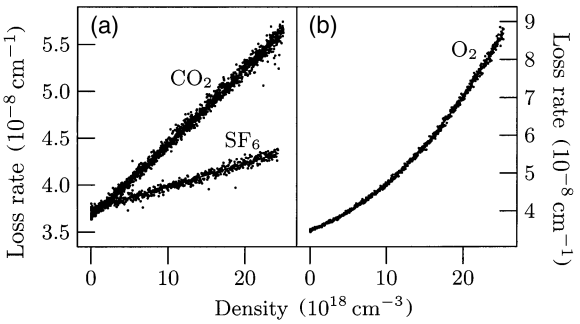

Fig. 2. Extinction measurements as a function of density. (a) CO_2 and SF_6 exhibit a linear density dependence at 197.99 nm. (b) O_2 shows a quadratic pressure dependence at 197.039 nm (50 751.4 cm^{-1}).

Table 1. Extinction Cross Sections for SF_6 and CO_2 at 197.99 nm (50 507.96 cm^{-1})[a]

Gas	Measured Cross Section (10^{-25} cm^2 mol^{-1})	Literature Value (10^{-25} cm^2 mol^{-1})
CO_2	86 ± 10	70[b]
SF_6	26 ± 4	23.6[c]

[a]Results are an average over several pressure scans.
[b]From an interpolation between values given in Ref. 8.
[c]Refractive index extrapolated from two points[9]; King factor assumed to be unity.[10]

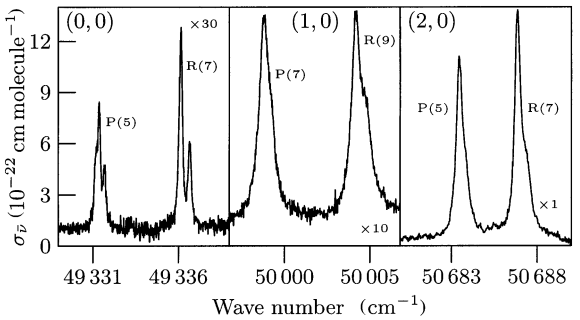

Fig. 3. Spectral recording of part of the $B\,^3\Sigma_u^- \leftarrow X\,^3\Sigma_g^-(v', 0)$ band in molecular oxygen. As the (0, 0) and (1, 0) bands are the weakest, those signals were multiplied with the indicated factor. All sections of the spectrum span 10 cm^{-1}. The (0, 0), (0, 1), and (0, 2) bands were measured at 2.90, 27.4, and 4.3 hPa, respectively.

Table 2. Extinction Cross Sections of O_2 in the Herzberg Continuum

Wavelength (nm)	Linear Contribution (10^{-24} cm^2 mol^{-1})	Quadratic Contribution (10^{-45} cm^5 mol^{-2})
This work		
197.039	6.6 ± 0.8	549 ± 15
197.518	8.4 ± 0.8	580 ± 15
199.743	7.0 ± 0.8	471 ± 15
Results from Coquart *et al.*[11]		
197.04	8.10 ± 0.14	521 ± 6
197.52[a]	8.0 ± 0.4	534 ± 20
197.76	8.04 ± 0.27	514 ± 16

[a]Interpolated value.

highly accurate determination of deep-UV resonance frequencies; the frequencies of the seed light were measured with an ATOS LM007 wavelength meter with an accuracy of 0.002 cm^{-1}, which was verified during the measurement campaign by calibration on I_2 hyperfine lines measured in saturation. Line positions of single resolved lines in the (0, 0) SR band could be determined to within 0.02 cm^{-1}. From a fit to the rotational structure involving 64 lines accurate values of the fine structure constants were determined. The spin–spin interaction constant λ is determined to be 1.642 ± 0.007 cm^{-1}, the centrifugal distortion of this constant λ_D is $(-4.0 \pm 1.1) \times 10^{-4}$ cm^{-1}, and the spin–rotation constant γ is $(-3.11 \pm 0.03) \times 10^{-2}$ cm^{-1}. Besides the three bands originating in the $X\,^3\Sigma_g^-, v'' = 0$ ground state, the (2, 1) band probing vibrationally excited population was also observed at room temperature overlapping the (0, 0) band. Phenomena of predissociation are associated with the linewidths, which can be seen to vary in Fig. 3 for the various v' levels. In future publications more details on the spectroscopy and on vibrational and spin-dependent predissociation rates (including a comparison with calculations in Ref. 12) will be presented.

In addition to absorption measurements on the SR resonance features, pressure-dependent extinction features were investigated in the Herzberg continuum of oxygen near 198 nm. The absorption in the Herzberg continuum in O_2 at wavelengths shorter than 240 nm is strongly modified by collisions connected to a change in the dipole moment of the molecule, which breaks the symmetry rule that otherwise disallows the transition.[11,13] This leads to an intensity of the continuum with a quadratic density dependence. The wavelength range 200–240 nm is important in atmospheric physics, as this falls between the absorption by ozone and the strong absorption of the SR bands. One CRDS-monitored pressure scan of O_2 is shown in Fig. 2(b) for a measurement at 197.039 nm. A fit to the pressure-dependent loss rate gives both the linear and a quadratic contribution to the extinction. The results for oxygen are listed in Table 2. Comparison with earlier measurements by Coquart *et al.*[11] shows reasonable agreement; Coquart *et al.* had a far lower resolution (~16 cm^{-1}) and needed to subtract the SR bands, whereas our resolution is much higher and resonances could be avoided.

In conclusion, the technique of cavity ringdown spectroscopy has been extended below 200 nm in the deep-UV range. The sensitivity is currently limited by the low reflectivity of available mirrors and could be improved once better mirrors can be produced. The CRD technique is demonstrated in measurements of extinction of various gas-phase molecules with a novel deep-UV pulsed laser source with a narrow bandwidth.

We gratefully acknowledge financial support from the Space Research Organization Netherlands and the Netherlands Foundation for Fundamental Research of Matter (FOM). M. Sneep's e-mail address is sneep@nat.vu.nl.

References

1. A. O'Keefe and D. Deacon, Rev. Sci. Instrum. **59,** 2544 (1988).
2. R. Engeln, E. van den Berg, G. Meijer, L. Lin, G. M. H. Knippels, and A. F. G. van der Meer, Chem. Phys. Lett. **269,** 293 (1997).
3. G. Berden, R. Peeters, and G. Meijer, Int. Rev. Phys. Chem. **19,** 565 (2000).
4. P. Zalicki, Y. Ma, R. N. Zare, E. H. Wahl, J. R. Dadamio, T. G. Owano, and C. H. Kruger, Chem. Phys. Lett. **234,** 269 (1995).
5. R. T. Jongma, M. G. H. Boogaarts, I. Holleman, and G. Meijer, Rev. Sci. Instrum. **66,** 2821 (1995).
6. H. Naus and W. Ubachs, Opt. Lett. **25,** 347 (2000).
7. H. Naus, I. H. M. van Stokkum, W. Hogervorst, and W. Ubachs, Appl. Opt. **40,** 4416 (2001).
8. M. Ogawa, J. Chem. Phys. **54,** 2550 (1971).
9. D. Vukovic, G. A. Woolsey, and G. B. Scelsi, J. Phys. D **29,** 634 (1996).
10. N. J. Bridge and A. D. Buckingham, Proc. R. Soc. London Ser. A **295,** 334 (1966).
11. M. Coquart, M.-F. Mérienne, and A. Jenouvrier, Planet. Space Sci. **38,** 287 (1990).
12. B. R. Lewis, S. T. Gibson, and P. M. Dooley, J. Chem. Phys. **100,** 7012 (1994).
13. A. J. Blake and D. G. McCoy, J. Quant. Spectrosc. Radiat. Transfer **38,** 113 (1987).